Using two-photon standing waves and patterned photobleaching to measure diffusion from nanometers to microns in biological systems

Sara K. Davis and Christopher J. Bardeen[a)]
Department of Chemistry, University of Illinois, 600 South Mathews Avenue, Urbana, Illinois 61801

(Received 25 September 2001; accepted for publication 31 January 2002)

A method of measuring molecular diffusion rates in microscopic sample volumes is described. This method utilizes the standing wave interference created by colliding two counterpropagating laser beams at the focus of two opposing microscope objectives, creating a periodic light distribution in a volume on the order of 1 fl. By using a Pockels cell to vary the laser intensity with a time resolution of milliseconds, we show how this experimental geometry can be used to perform ultrahigh resolution fluorescence recovery after patterned photobleaching (FRAPP) experiments. A mathematical treatment of the experiment shows that the laser excitation profile has two characteristic length scales, the width of the focal spot and the period of the standing wave, which permits the simultaneous measurement of dynamics on two separate length scales. This feature may be used to determine whether the measured diffusion is anomalous. We present experimental results using a femtosecond Ti:sapphire laser to create a two-photon excitation profile with a fringe visibility on the order of 100. This standing wave is used to demonstrate FRAPP in both model dye/polymer systems and in more complex systems like living cells stained with a fluorescent dye. By combining the advantages of standing wave microscopy and two-photon fluorescence recovery after photobleaching, this technique permits the measurement of very short length motions in localized sample volumes, which should be useful in both biology and the study of diffusion in microscopically heterogeneous systems.
[DOI: 10.1063/1.1464656]

I. INTRODUCTION

How molecules move in living cells is an important area of research in biology. Despite extensive study, the relative importance of active versus diffusive transport, the role of molecular crowding and anomalous diffusion, and the role of the cytoarchitecture (e.g., actin filaments) remain largely unknown. Many different experimental methods have been used to observe motion in biological systems, from nuclear magnetic resonance studies on water diffusion in macroscopic samples[1] to more localized experiments like fluorescence correlation spectroscopy (FCS),[2] single particle tracking,[3] and fluorescence recovery after photobleaching (FRAP).[4] This last method is often used to measure diffusion due to its high temporal resolution and ability to probe spatially localized subcellular regions. In a FRAP experiment, specific components of the cell are stained by a fluorescent dye. By using a microscope objective, one can focus a laser down to a spot on the order of 1 μm or less at visible wavelengths, and then briefly increase the laser power by several orders of magnitude, destroying a significant fraction of absorbing molecules in the focal region. After the photobleaching pulse, the fluorescence signal recovers due to diffusion of unbleached molecules from outside the spot into the laser focus. This recovery is monitored by fluorescence excited by a weak probe beam, and it is straightforward to obtain a diffusion constant from the shape of the recovery.[4] In this way, diffusive motion can be measured on microsecond time scales and submicron length scales, although the highest resolution measurements require focusing the laser down to the diffraction limit. In this case the beam profile can no longer be approximated as a simple Gaussian, and the analysis becomes more complicated.[4]

There have been two important extensions of the FRAP technique as originally developed by Webb and co-workers. The first was the recognition that using a periodic bleach pattern, rather than a single spot, could improve the experimental signal to noise, remove artifacts due to probe photobleaching, and simplify the data analysis.[5–7] In FRAPP, the interference of two beams creates a fringe pattern in the sample. After photobleaching the interference pattern into the stained sample, a weak probe fringe pattern is scanned across the sample by varying the phase of one of the interfering beams. The resulting fluorescence signal oscillates with the phase of the probe grating until the fringe pattern of bleached dye molecules washes out due to diffusion. Advantages of the FRAPP experiment include: (1) the decaying signal is oscillatory, allowing sensitive methods like lock-in detection to be used; (2) the decay of the signal has a simple exponential dependence on the diffusion constant; and (3) the signal is insensitive to artifacts arising from probe bleaching of the sample, which in FRAP experiments can lead to longer apparent fluorescence recovery times. Despite its advantages, the use of FRAPP has not become as widespread as that of the simple FRAP technique. One reason is that it is more difficult to implement experimentally. A sec-

a)Author to whom correspondence should be addressed; electronic mail: bardeen@scs.uiuc.edu

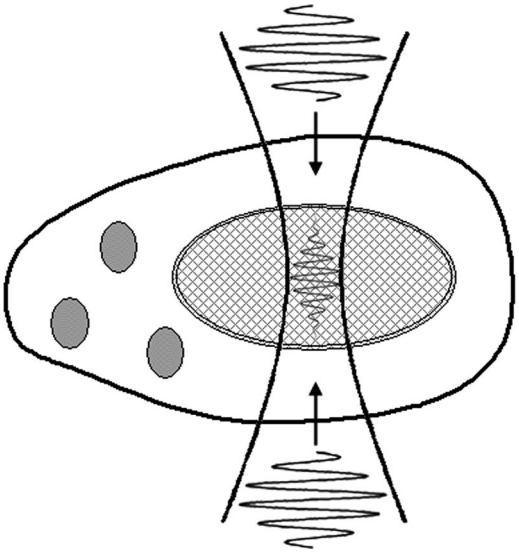

FIG. 1. Schematic of experiment. Pulses from two counterpropagating laser beams are focused into the sample, creating a standing wave interference pattern at the focus.

ond, more fundamental reason is that it lacks the localized nature of spot FRAP. In order to establish the requisite fringe pattern, the two interfering beams are crossed at an angle and the illuminated spot contains many fringes, resulting in a measurement of diffusion averaged over a larger area of the sample. A second improvement in FRAP is the use of multiphoton excitation and probing.[8,9] The intrinsic three-dimensional confinement of the two-photon excitation profile allows the straightforward measurement of diffusion in the interior of live cells, without the need for confocal pinholes. The other advantage of using two-photon excitation is the increased cell viability under near infrared illumination as opposed to visible illumination.[10]

In the present article we describe a combination of two-photon excitation and patterned photobleaching which takes full advantage of both approaches. In order to maximize the spatial resolution of the FRAPP experiment, we employ a standing wave geometry,[11] where two counterpropagating laser pulses collide in the sample to create a patterned two-photon photoexcitation profile localized to a volume of a few femtoliters. In the present article we outline the theoretical basis for the experiment and data analysis, the experimental setup, and show examples of how this technique can be applied to the diffusion of fluorescently labeled DNA in live XTC-2 cells. The advantages of the two-photon standing wave FRAPP experiment include high spatial resolution and a clear way to analyze the data for effects like anomalous diffusion. Finally, the ability to create a stable two-photon standing wave inside a living cell provides the opportunity of making other types of high resolution interferometric measurements, from traveling wave FCS[12–14] to high precision measurements of the distance between two fluorescently labeled objects.[15]

II. THEORY

Figure 1 shows a schematic picture of the experiment, where two counterpropagating laser pulses collide in the sample, creating a temporary standing wave that provides the periodic excitation profile. The intensity profile for two equal intensity counterpropagating Gaussian laser beams can be written as

$$I(x,y,z)=\frac{2}{\pi}\frac{P}{W(z)^2}\exp\left[\frac{-2(x^2+y^2)}{W(z)^2}\right]\times\left(1+\cos\left(\frac{2\pi z}{\Lambda}\right)\right), \tag{1}$$

where

$$W(z)=w_0\sqrt{1+\left(\frac{z}{z_R}\right)^2}$$

describes the axial dependence of the beam radius and $z_R=\pi {w_0}^2/\lambda$ is the Rayleigh range. P is the power of each beam, n is the index of refraction of the medium, λ is the wavelength of light, $\Lambda=\lambda/2n$ is the peak to peak fringe spacing, and w_0 is the beam diameter at the focus. The two-photon excitation profile is proportional to the intensity squared and can be written as

$$I^2(x,y,z)=\frac{2}{\pi^2}\frac{P^2}{W(z)^4}\exp\left[\frac{-4(x^2+y^2)}{W(z)^2}\right]\times\left(3+4\cos\left(\frac{2\pi z}{\Lambda}\right)+\cos\left(\frac{4\pi z}{\Lambda}\right)\right). \tag{2}$$

For small focal volumes, the axial dependence of this expression can be approximated by replacing the $W(z)$ dependence with a Gaussian decay,[9] which serves to confine the excitation profile along the z axis

$$I^2(x,y,z)\cong\frac{2}{\pi^2}\frac{P^2}{w_0^4}\exp\left[-\frac{4(x^2+y^2)}{w_0^2}-\frac{2z^2}{d^2}\right]\times\left(3+4\cos\left(\frac{2\pi z}{\Lambda}\right)+\cos\left(\frac{4\pi z}{\Lambda}\right)\right), \tag{3}$$

where d is an adjustable parameter set by experimental measurement of the axial dependence of the two-photon excitation probability. To a first approximation d is identical to the Rayleigh range z_R. The initial concentration of chromophores, assumed to be homogeneously distributed in the sample, is

$$C(x,y,z)=C_0. \tag{4}$$

In the limit of relatively weak (<30%) photobleaching, the change in concentration is linearly proportional to the excitation probability, and the concentration profile immediately after two-photon photobleaching is approximated by

$$C(x,y,z,t=0)=C_0(1-\sigma I^2(x,y,z)), \tag{5}$$

where σ is the nominal bleach depth. The solution to the diffusion equation with this initial condition can be obtained by convoluting this initial concentration profile with a diffusion function

$$\mathrm{Diff}(x,y,z,t)=\frac{1}{8(\pi Dt)^{3/2}}\times\exp\left[-\frac{x^2+y^2+z^2}{4Dt}\right], \tag{6}$$

where D is the diffusion coefficient. If we make the approximation that $Dt\ll d^2$, which basically constrains the applicability of Eq. (7) to times shorter than the time it takes a particle to diffuse across the Rayleigh range of the focused beam, we find that the time dependent concentration profile that contains both an oscillatory and a non-oscillatory component

$$\begin{aligned}C(x,y,z,t)&=C(x,y,z,0)\otimes\mathrm{Diff}(x,y,z,t)\\&\cong C_0\left\{1-\sigma\frac{w_0^2}{w_0^2+16Dt}\exp\left[-\frac{x^2+y^2}{4Dt+w_0^2/4}\right]\right.\\&\quad\times\left(3+4\exp\left[-\frac{4\pi^2Dt}{\Lambda^2}\right]\cos\left(\frac{2\pi z}{\Lambda}\right)\right.\\&\quad\left.\left.+\exp\left[-\frac{16\pi^2Dt}{\Lambda^2}\right]\cos\left(\frac{4\pi z}{\Lambda}\right)\right)\right\}.\end{aligned} \tag{7}$$

This evolving concentration profile can be probed using a second two-photon standing wave which is translated along the z axis by varying its phase ϕ. As the fringes move in and out of phase, the fluorescence signal will alternately increase and decrease. The total fluorescence detected is proportional to the product of the concentration with the intensity squared, integrated over all space

$$\mathrm{Sig}(t,\phi)\propto\int_{-\infty}^{\infty}dx\int_{-\infty}^{\infty}dy\int_{-\infty}^{\infty}dz\,C(x,y,z,t)I^2(x,y,z,\phi). \tag{8}$$

Again making the approximation that $Dt\ll d^2$, we obtain

$$\begin{aligned}\mathrm{Sig}(t,\phi)&\cong C_0\left\{1-\sigma'\frac{w_0^2}{w_0^2+8Dt}\left(18+16\right.\right.\\&\quad\times\exp\left[-\frac{4\pi^2Dt}{\Lambda^2}\right]\cos(\phi)\\&\quad\left.\left.+\exp\left[-\frac{16\pi^2Dt}{\Lambda^2}\right]\cos(2\phi)\right)\right\},\end{aligned} \tag{9}$$

where σ' is a constant that is proportional to the bleach depth and ϕ is the variable phase of the probe beam that results in a spatial translation of the standing wave. The full expression for Eq. (9), with its dependence on the axial distance d, is straightforward to derive but cumbersome. In the present work, we are interested mainly in the decay of the $\cos(\phi)$ term, which occurs when a particle diffuses from a peak to a valley in the interference pattern. Equation (9) is valid when the inequality

$$Dt\ll d^2 \tag{10}$$

is satisfied. Since the Rayleigh range is proportional to the beam waist, this means that the beam cannot be focused too tightly, or the inequality that justifies Eq. (9) will break down. If we are interested in the decay of the oscillations to $1/e$ of their initial amplitude, then inequality (10) implies

$$D\tau_{\mathrm{osc}}=\frac{\Lambda^2}{4\pi^2}\ll d^2\approx\left(\frac{\pi w_0^2}{\lambda}\right)^2\Rightarrow\frac{\lambda^4}{16\pi^4n^2}\ll w_0^4. \tag{11}$$

If we are interested in the time it takes the bleach to recover by 50%, then we have

$$D\tau_{1/2}=\frac{w_0^2}{8}\ll d^2\approx\left(\frac{\pi w_0^2}{\lambda}\right)^2\Rightarrow\frac{\lambda^2}{8\pi^2}\ll w_0^2. \tag{12}$$

In the experiments in this article, we have $\lambda=800$ nm and $n=1.45$ (cytoplasm), and a two-photon excitation radius w_0 of approximately 1.2 μm. These values mean that inequalities (11) and (12) are both satisfied, and Eq. (9) should describe our experiments. In general, the beam may be focused to within a factor of 2 of the diffraction limit and still fulfill inequality (10).

Equation (9) contains three types of time dependent terms: the $\cos(2\phi)$ term, which makes a small contribution to the overall signal and decays rapidly; the $\cos(\phi)$ term which decays with a characteristic time of $\Lambda^2/4\pi^2D$ (the standard result for a FRAPP experiment); and a non-oscillatory component which recovers with a half life of $w_0^2/8D$ (the standard result for a two-photon spot FRAP experiment). Neglecting the $\cos(2\phi)$ term, which is difficult to discern in the signal to noise of a real experiment, the standing wave FRAPP experiment then allows us to measure diffusion on two length scales simultaneously. The first length scale is the fringe spacing Λ, while the second is the beam diameter w. By varying the spot size w, we can make the relative size of these two length scales arbitrarily large. The characteristic time scales are proportional to the squares of the length scales

$$\frac{\tau_{1/2}}{\tau_{\mathrm{osc}}}=\left(\frac{w_0}{\lambda}\right)^2 2n^2\pi^2 \tag{13}$$

and typically in our experiments the beam diameter is about four times larger than the fringe spacing, so the characteristic time scales for diffusion differ by a factor of 100.

This separation of time scales is particularly useful if anomalous diffusion is suspected in the data. In biological systems, where the solvent has a very high concentration of macromolecules, it is possible that the conditions necessary for simple diffusion are not fulfilled and the root mean square displacement does not grow linearly with time. In this case the diffusion is termed anomalous.[16] If the system still obeys Gaussian statistics, the diffusion function may be modified to take this into account:[17]

$$\mathrm{Diff}(x,y,z,t)=\frac{1}{8(\pi Dt^{\alpha})^{3/2}}\times\exp\left[-\frac{x^2+y^2+z^2}{4Dt^{\alpha}}\right], \tag{14}$$

where $\alpha>1$ leads to superdiffusion and $\alpha<1$ leads to subdiffusion. In this case Eq. (6) becomes

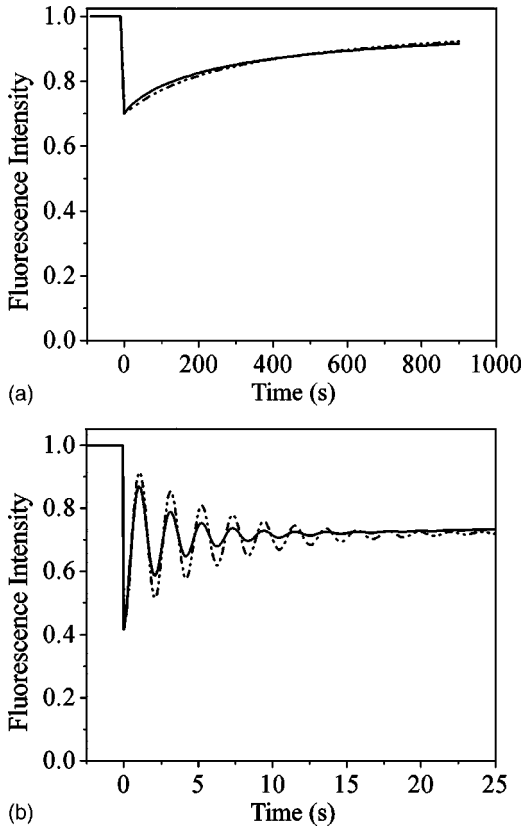

FIG. 2. (a) Fluorescence recovery after photobleaching, calculated using Eq. (9) with the ratio $w/\Lambda=2$. Solid curve is $\alpha=0.85$ and $D=0.0010\ \mu m^2/s$, dashed curve is $\alpha=1.0$ and $D=0.0004\ \mu m^2/s$. (b) Short time dynamics of curve in (a) showing oscillatory decay due to nanometer diffusion along the z axis.

$$\mathrm{Sig}(t,\phi)\approx C_0\left\{1-\sigma'\frac{w_0^2}{w_0^2+8Dt^\alpha}\times\left(18+16\exp\left[-\frac{4\pi^2Dt^\alpha}{\Lambda^2}\right]\cos(\phi)+\exp\left[-\frac{16\pi^2Dt^\alpha}{\Lambda^2}\right]\cos(2\phi)\right)\right\}. \quad (15)$$

In biological systems, subdiffusion is the most likely possibility, and several experiments have found evidence for this in the long-time decays of their FRAP data.[9,18,19] These previous experiments rely on a single observable to obtain both short and long time decay dynamics, and the signal to noise limits the accuracy to which data at the extremes can be analyzed. In standing wave FRAPP, both the short time diffusion, which washes out the interference fringes, and the long time decay, which fills in the bleach, can be accurately measured in the same experiment. Figure 2 shows an example relevant to our experimental setup, where the ratio $w_0/\Lambda=2$ and the two decay curves are plotted with different time axes for two values of α and D, both of which fit the long-time bleach recovery well, but give clearly different results for the short-time oscillation decay. Thus even if the detailed fitting of the bleach recovery is ambiguous, the oscillatory decay provides a way to check the fitting parameters in a completely different time regime. A difference in the time scales of the two decays is a clear indication that the diffusion ''constant'' is actually time dependent and that the diffusion is anomalous.

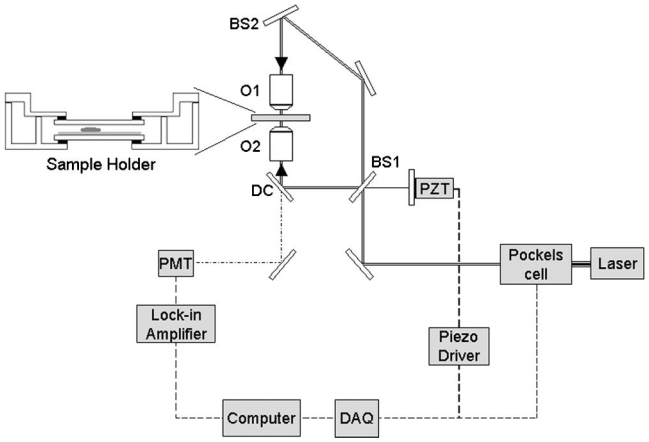

FIG. 3. Experimental setup. A 90 MHz Ti:sapphire laser generates ~45 fs, 800 nm pulses. The intensity of the beam is regulated with a Pockels cell. A prism compressor (not shown) compensates for chirp in the pulses. The beam is split at BS1. Half of the beam is directed by a mirror and a second beam splitter (BS2) into the back of a microscope objective (O1) and is focused onto the sample. The other half of the beam is reflected onto a mirror attached to a piezoelectric actuator (PZT) and back through BS1. The beam is then reflected by a dichroic mirror (DC) into the back of the second objective (O2) and is focused onto the sample. Fluorescence from the sample is collected by O2, transmitted through the DC and then directed into the PMT. The signal from the PMT is collected by a lock-in amplifier and recorded by a computer. The computer controls the piezo driver and the Pockels cell with a DAQ board. The biological sample holder has two aluminum pieces. A collagen gel-coated coverslip with attached cells is affixed to the bottom piece of the sample holder with a thin layer of vacuum grease. A clean coverslip is attached to the top piece in the same manner. Raised columns on two sides of the bottom coverslip provide support while allowing flow of medium throughout the chamber.

In the above treatment, we have neglected the effects of molecular rotation and reversible photobleaching on the observed signal. If these effects occur on the time scale of the experiment, they can lead to an apparent decay in the oscillations, which is not due to translational motion but rather to either rotation of a transition dipole or intramolecular chemistry. Such intramolecular dynamics do not depend on the length scale of measurement, and in this case the rate of oscillation decay will be the same as that of the full bleach recovery. We have observed dynamics of this nature for dye molecules in plasticized polymers (data not shown). A clear separation of the time scales for oscillation decay and bleach recovery was observed in all the experiments presented in this article, indicating that rotation and reversible photobleaching did not affect the data.

III. EXPERIMENT

A schematic outline of the experimental setup is shown in Fig. 3. A laser system consisting of a 90 MHz Ti:sapphire oscillator (Kapteyn-Murnane Labs) pumped by a diode-pumped frequency-doubled Nd-YVO_4 laser generates ~45 fs, 800 nm pulses, which pass through a prism compressor (not shown) to compensate for linear chirp from the optics. The intensity of these pulses is varied by a Pockels cell (Conoptics 350-50) which is electronically switched by the

output of a computer data acquisition (DAQ) board (National Instruments PCI-6024E). The beam is divided by a beam splitter (BS1) upon entry into the microscope setup. One part is reflected to a mirror attached to a piezo driven translation stage (Thorlabs MDT691 and AE0505D16) whose movement is controlled to better than 10 nm precision by the output of the computer DAQ board. This beam is reflected back through BS1 and into the laser port of an inverted microscope (Olympus IX-70), where it is directed upward through the bottom objective by a dichroic mirror. The second part of the laser beam is reflected into the top objective by another 50/50 beam splitter (BS2) to equalize the beam intensities. Both beams are focused onto the sample, spatially overlapped using adjustable mirror mounts, and temporally overlapped using an actuator attached to the piezo stage. The optics in the interferometer are bolted to vibrationally damped stainless steel posts (Thorlabs P14), which in turn are bolted to the laser table along with the microscope itself.

In order to create a standing wave in the collagen-supported cells, optical access from both the top and bottom is required. The aluminum sample holder shown in Fig. 3 allows a coverslip containing the biological sample to be placed within a few hundred microns of the top coverslip while allowing medium to circulate over the cells from reservoir chambers on the sides. A water-tight seal between the coverslips and the aluminum is created using a thin film of vacuum grease. With the sample holder sealed tightly with parafilm, XTC-2 cells remain viable for up to 5 days as determined by their ability to reproduce. The cells themselves are supported on a layer of collagen ranging from 10 to 100 μm, which provides an index-matched spacer between the confocal region and any interface (e.g., glass–water) that could lead to spurious reflections.

The beams are focused by two $40\times$ 0.66 numerical aperture Leica microscope objectives, and the input beam diameter is adjusted with a Galilean telescope before the microscope to underfill the rear aperture of the objectives, resulting in spot sizes tunable from 1 to 2.5 μm in diameter as measured by both direct imaging the two-photon fluorescence spot and translation of a fluorescent bead through the spot. The two-photon fluorescence is collected by the bottom objective and directed into a photomultiplier tube (PMT) (Hamamatsu R1527P). A hot mirror and a BG28 filter are used to eliminate any infrared background from the fluorescence signal. The peak beam intensity at the focus was 4×10^{9} W/cm^2 for the probing beam and 5×10^{10} W/cm^2 for the bleaching beam. In addition to two-photon absorption, direct one-photon absorption of water at 800 nm can lead to thermal heating of the sample volume. Calculations of this effect lead to an upper limit of the temperature change in the focal volume of 0.3 °C, in agreement with previous estimates of two-photon heating in the focus of an objective lens.[20]

The signal may be collected in several different modes. One obvious method is to translate the piezo back and forth at a fixed frequency and use lock-in detection to detect the oscillatory signal at that frequency.[6,7,11] This method takes advantage of the phase sensitive detection of the lock-in, but has the disadvantage that the signal is very sensitive to phase drifts in the interferometer,[11,21] which has large path lengths and is suspended above the laser table. It also is sensitive only to the oscillatory component, since the lock-in output contains no information about the decay of the non-oscillatory component. A second approach is to use an analog to digital board, boxcar, or lock-in amplifier where the entire signal is modulated by an external chopper, and then record the PMT signal as a function of time. Subsequent data analysis can then extract the magnitudes of the oscillatory and non-oscillatory components, making full use of the information content of the signal. For the experiments presented in this article, we use the latter method with a lock-in amplifier (Stanford Research Systems SR830 DSP), and our data traces show the full signal as the piezo is scanned back and forth. This back and forth scanning leads to abrupt phase changes in the signal, so we analyze the data by taking each subset of data that corresponds to an uninterrupted motion of the piezo and extract an amplitude of oscillation by either Fourier transform methods or simple measurement of the average maximum/minimum visibility of the signal after the data have been smoothed to remove high frequency noise.

For the experiments on live cells, we grow *Xenopus* XTC-2 cells in phenol red-free DME/F12 medium (Sigma) supplemented with 10% fetal bovine serum at room temperature. Collagen gel is made by combining 778 μl of the above medium with 222 μl rat tail collagen (type I) (Upstate Biotechnology) dissolved in 0.1 N acetic acid. The mixture is chilled on ice and then 14 μl of chilled 0.5 N NaOH is added. The final solution is kept on ice until use. 300 μl of the collagen solution is pipetted onto a 50×45 mm microscope coverslip in a Petri dish. The solution is spread evenly over the surface of the coverslip and then allowed to gel for 15 min in a 37 °C incubator. Collagen gel-coated coverslips are kept immersed in medium at room temperature until use. Cells are resuspended in medium and then seeded onto the collagen gel, where they are allowed to plate for a minimum of 4 h before staining. To stain the cells, the gel-coated coverslips with attached cells are gently rinsed with a solution of 70% phosphate buffered saline (PBS) (BioWhittaker) in water. Cells are stained for 10 min at room temperature in a 9 μM solution of Hoechst 33342 (Sigma) in 70% PBS. After staining, the samples are gently rinsed five times with 70% PBS, and then covered with medium. Petri dishes containing the samples are parafilmed and stored at room temperature until use.

IV. RESULTS

In order to experimentally measure the two-photon standing wave profile, we use an ultrathin two-photon detector comprised of a 50 nm thick film of the luminescent conjugated polymer poly(p-phenylene vinylene) (PPV) sandwiched between two microscope coverslips. We place this sample between the two microscope objectives, and by moving the piezo-mounted mirror we can translate the standing wave through the sample. The fluorescence signal shown in Fig. 4 goes up and down as the two-photon excitation peaks and valleys move across the sample. Note that the phase of the oscillations reverses as the piezo reverses direction and scans back and forth. The fringe visibility is close to unity,

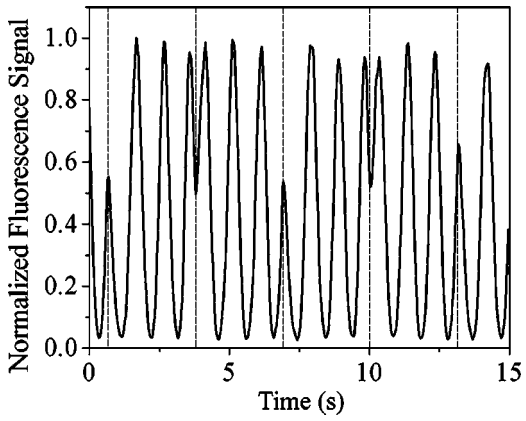

FIG. 4. Two-photon standing wave profile, obtained by scanning the phase of one of the beams, which translates the standing wave across a 50 nm thick fluorescent PPV film. Dashed lines indicate time at which the piezo direction was switched.

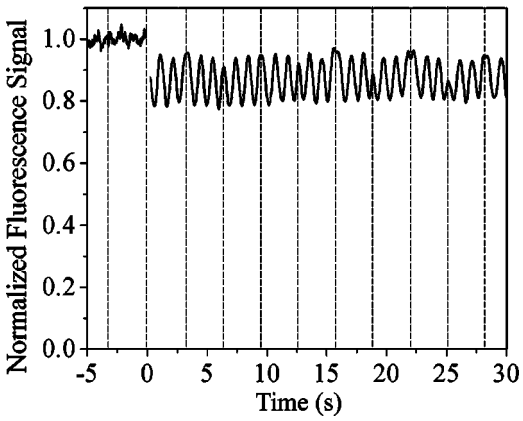

FIG. 5. Data from bleach of Rhodamine B in a thick PVA film. Prebleach scan ($t=-5-0$ s) shows no oscillations. At $t=0$ s, the laser intensity is increased for a duration of 50 ms, which bleaches the fringe pattern into the sample. This fringe pattern results in oscillations when the standing wave is translated again. Dashed lines indicate time at which the piezo direction was switched.

with the ratio of maximum to minimum being on the order of 30. This compares favorably to one-photon standing waves measured with ultrathin photodiodes[22] and is comparable to that measured by Hell and co-workers in their 4Pi microscopy setup.[23] The fringes are stable on the order of minutes before small phase jumps due to nanometer scale changes in the path length lead to drift on the order of half a wavelength.

We can use this two-photon standing wave to photobleach a standing wave pattern in a stationary system. By mixing Rhodamine B dye with polyvinyl alcohol in water, we make a spin-coated polymer film that exhibits two-photon fluorescence. These films are on the order of 10 μm thick, and so translating the standing wave through the sample does not result in any detectable oscillations in the fluorescence signal. If we then fix the standing wave and briefly increase its intensity, destroying a fraction of the Rhodamine molecules, the standing wave pattern is imprinted on the sample. This pattern can now be observed when the piezo stage is moved and translates the two-photon standing wave across the sample again. The decreased fluorescence signal shows deep oscillations due to the standing wave bleach, which persist for an indefinite amount of time since Rhodamine B is essentially frozen in the solid polymer. This sequence of events is shown in Fig. 5. It is important to point out that the experimental oscillations are not as pronounced as those predicted by Eq. (9), which assumed perfect fringe visibility and no phase drift. Imperfect alignment, sample inhomogeneity, and phase drift during the bleach period all contribute to a reduction in contrast of the bleach pattern. In addition, if the bleach power is too high, the two-photon absorption can become nonlinear due to Beer's law, leading to saturation in the bleach level and visibility of the oscillations. From our observations, the main contributor to the loss of fringe visibility is sample tilt and nonparallelism of the top and bottom surfaces that leads to small misalignments of the top beam relative to the bottom beam. In the case of the thin PPV sample, we can conveniently optimize the alignment using the fringe visibility, but for thicker samples there is no way to know in advance whether the alignment of the two beams is absolutely perfect—only after the bleaching experiment is there a quantitative indication of whether the alignment is correct.

Live cells are even more inhomogeneous than drop cast polymer films, but previous workers have demonstrated that it is possible to create a standing wave in this environment. Lanni and co-workers have used one-photon standing wave microscopy[24] to obtain high-resolution imaging of actin filaments,[25] and Hell and co-workers had previously demonstrated that two-photon standing waves inside fixed cells can also be used for static imaging.[26] Our experiments use cultured XTC-2 toad tissue cells, plated on a collagen matrix inside the sample holder shown in Fig. 3. We repeat the scan–bleach–scan sequence described above, and typical data, along with a transmitted light image of the particular cell that produced the data, are shown in Fig. 6. Unlike the dye molecules in solid polyvinyl alcohol (PVA), here the fringe oscillations die out within seconds due to the mobility of the chromatin DNA in live cells.[3,27] Binding and unbinding of the Hoechst 33342 (H33342) to the nuclear DNA makes a negligible contribution to the observed dynamics, as can be seen in Fig. 7. Here we have fixed the cells by treating them with formaldehyde, killing them, and crosslinking the proteins in order to lock the macromolecular structure in place. If they are now stained with H33342, we see that the fringe oscillations persist for tens of minutes as opposed to a few seconds. In the fixed cells, the only contribution to the diffusional dynamics is the motion of unbound H33342 molecules, or those that undergo a release–diffuse–rebind sequence.[28] Clearly this occurs on a much longer time scale than that observed in the experiments on live cells.

From the data shown in Fig. 6, we can fit the temporal shape of the oscillation amplitude to an exponential decay and extract a diffusion coefficient using Eq. (6). By averaging decay curves from 20 different cells, we obtain an average diffusion constant of 5×10^{-12} cm^2/s for DNA in live XTC-2 cells. This value is close to that obtained for chromatin motion observed in two different cell types using high resolution single particle tracking methods.[3] Given this diffusion constant and a spot size of 1.2 μm, we can calculate a

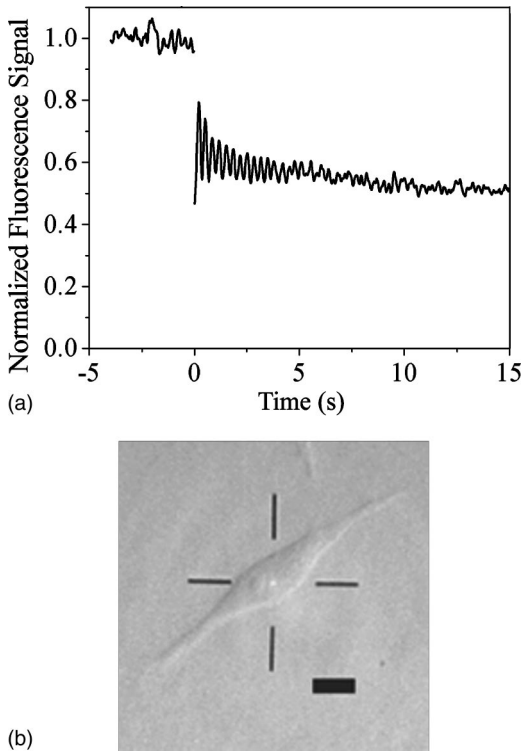

FIG. 6. Chromatin diffusion in XTC-2 Cell. (a) Data from bleach of Hoechst dye-stained nucleus of XTC-2 cell. Prebleach ($t=<0$ s) shows no oscillations. At $t=0$ s, a 50 ms duration jump in intensity bleaches the fringe pattern into the sample. Diffusion of chromatin causes the oscillations to decay over time. The direction of the piezo was switched every 0.66 s. (b) Transmitted light image of the XTC-2 cell for part (a). The bright spot at the center of the crosshairs is Hoechst fluorescence from laser excitation. Bar $=10\ \mu$m.

half life for the unmodulated fluorescence recovery of 6 min. In the cells we have studied, however, this FRAP recovery is not the simple recovery predicted by Eq. (9). In general, we see two types of behavior. In about 50% of the cells, we observe no change in the bleach on a time scale of 10–20 min, during which we would expect to see a recovery based on the diffusion constant obtained from the oscillatory decay. This lack of recovery is consistent with previous FRAP experiments on mammalian fibroblast cells,[28] suggesting that the diffusion is indeed anomalous in the sense that the DNA is constrained to move only within a small region of the nucleus. In the other 50% of the cells, however, the fluorescence signal seems to drift randomly, both up and down, over the course of minutes. This drift often occurs in spurts—the signal will be stable for several minutes, then suddenly increase or decrease. These fluctuations are probably due to larger scale motions of the chromatin in the nucleus, and we are currently studying the origin of this behavior using high resolution fluorescence imaging of the entire cell. The lack of consistent long-time behavior in these cells, however, makes extracting a second diffusion coefficient problematic.

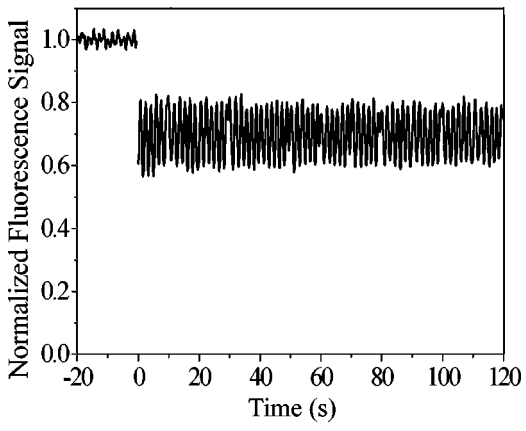

FIG. 7. Data from bleach of XTC-2 cell after treatment with formaldehyde. Prebleach ($t=<0$ s) shows no oscillations. At $t=0$ s, a 50 ms duration jump in intensity bleaches the fringe pattern into the sample. The direction of the piezo was switched every 10 s. Note that the time scale for this scan is significantly longer than that shown in Fig. 6.

Two-photon standing wave FRAPP combines the advantages of high spatial resolution, localized photoexcitation, and straightforward data analysis in a single experiment. It adds a new dimension to previously developed two-photon FRAP techniques and should permit easier analysis of anomalous diffusion in biological systems. Although our measurements concern relatively slow dynamics on a time scale of seconds, the method can be extended to much shorter time scales through the use of faster detection methods like high speed data acquisition devices and fast phase modulators like resonantly driven piezo-electric scanners[29] or electro-optic phase modulators.[14] In principle, its temporal resolution is limited only by the experimental ability to acquire data with sufficient signal to noise to detect recovery of the amplitude of the oscillations. The experimental setup is compatible with conventional microscopy experiments, making it easy to switch between regular microscopy of the sample and the time-resolved FRAPP experiment. Finally, we have demonstrated the application of this technique to live cells and are using its unique capabilities to learn more about molecular motions in living systems.

ACKNOWLEDGMENTS

The authors acknowledge the assistance of Drew Stout in constructing the experimental apparatus, and the help of the School of Chemical Sciences Cell Media Facility. They also acknowledge support from a Research Corporation Research Innovation Award, and the University of Illinois Research Board.

[1] A. I. Garcia-Perez, E. A. Lopez-Beltran, P. Kluner, J. Luque, P. Ballesteros, and S. Cerdan, Arch. Biochem. Biophys. **362**, 329 (1999).
[2] D. Magde, E. Elson, and W. W. Webb, Phys. Rev. Lett. **29**, 705 (1972).
[3] W. F. Marshall, A. Straight, J. F. Marko, J. Swedlow, A. Dernburg, A. Belmont, A. W. Murray, D. A. Agard, and J. W. Sedat, Curr. Biol. **7**, 930 (1997).
[4] D. Axelrod, D. E. Koppel, J. Schlessinger, E. Elson, and W. W. Webb, Biophys. J. **16**, 1055 (1976).
[5] B. A. Smith and H. M. McConnell, Proc. Natl. Acad. Sci. U.S.A. **75**, 2759 (1978).
[6] J. Davoust, P. F. Devaux, and L. Leger, EMBO J. **1**, 1233 (1982).
[7] F. Lanni and B. R. Ware, Rev. Sci. Instrum. **53**, 905 (1982).
[8] W. Denk, J. H. Strickler, and W. W. Webb, Science **248**, 73 (1990).
[9] E. B. Brown, E. S. Wu, W. Zipfel, and W. W. Webb, Biophys. J. **77**, 2837 (1999).
[10] J. Squier and M. Muller, Rev. Sci. Instrum. **72**, 2855 (2001).

[11] M. T. Cicerone, F. R. Blackburn, and M. D. Ediger, Macromolecules **28**, 8224 (1995).
[12] M. Hattori, H. Shimizu, and H. Yokoyama, Rev. Sci. Instrum. **67**, 4064 (1996).
[13] R. L. Hanson, X. R. Zhu, and J. M. Harris, Anal. Chem. **70**, 1281 (1998).
[14] D. Margineantu, R. A. Capaldi, and A. H. Marcus, Biophys. J. **79**, 1833 (2000).
[15] M. Schmidt, M. Nagorni, and S. W. Hell, Rev. Sci. Instrum. **71**, 2742 (2000).
[16] M. Saxton, Biophys. J. **56**, 615 (1989).
[17] K. G. Wang and M. Tokuyama, Physica A **265**, 341 (1999).
[18] P. Schwille, U. Haupts, S. Maiti, and W. W. Webb, Biophys. J. **77**, 2251 (1999).
[19] O. Seksek, J. Biwersi, and A. S. Verkman, J. Cell Biol. **138**, 131 (1997).
[20] A. Schonle and S. W. Hell, Opt. Lett. **23**, 325 (1998).
[21] B. M. Hoeling, A. D. Fernandez, R. C. Haskell, E. Huang, W. R. Myers, D. C. Petersen, S. E. Ungersma, R. Wang, and M. E. Williams, Opt. Express, **6**, 136 (2000).
[22] M. Sasaki, X. Mi, and K. Hane, Appl. Phys. Lett. **75**, 2008 (1999).
[23] M. Schrader, U. G. Hofmann, and S. W. Hell, J. Microsc. **191**, 135 (1998).
[24] B. Bailey, D. L. Farkas, D. L. Taylor, and F. Lanni, Nature (London) **366**, 44 (1993).
[25] V. C. Abraham, V. Krishnamurthi, D. L. Taylor, and F. Lanni, Biophys. J. **77**, 1721 (1999).
[26] M. Schrader, K. Bahlmann, G. Giese, and S. W. Hell, Biophys. J. **75**, 1659 (1998).
[27] H. Bornfleth, P. Edelmann, D. Zink, T. Cremer, and C. Cremer, Biophys. J. **77**, 2871 (1999).
[28] J. R. Abney, B. Cutler, M. L. Fillbach, D. Axelrod, and B. A. Scalettar, J. Cell Biol. **137**, 1459 (1997).
[29] B. M. Hoeling, A. D. Fernandez, R. C. Haskell, and D. C. Petersen, Rev. Sci. Instrum. **72**, 1630 (2001).